Influence of the solvent removal method on the morphology of polystyrene porous structures prepared via thermally induced phase separation

Patrik Boura[1,2] · Alexandr Zubov[1] · Bart Van der Bruggen[2] · Juraj Kosek[1]

Abstract

Thermally induced phase separation (TIPS) allows preparation of nano and micro-porous structured materials for various applications. The literature thoroughly examines the impact of initial polymer solution concentration and cooling rate on the products morphology. On the contrary, the influence of the solvent removal methods was so far researched scarcely. Hence, we compare both qualitatively and quantitatively the effects of the solvent removal method on pore size distribution, structure, porosity, and thermal conductivity. Our study was carried out with samples prepared by TIPS from polystyrene/cyclohexane solutions employing either extraction agent or lyophilization at different solvent removal temperatures. Materials exhibited interconnected pore structure, implying good sound insulation properties, and had low thermal conductivity, offering the combination of thermal and sound insulation in one layer of material. Pore sizes after lyophilization were up to two times larger than after solvent removal by an extraction agent. On the other hand, the use of extraction agent led up to 10% porosity decrease with average porosity after lyophilization being above 82%. Our findings demonstrate that the solvent removal method is an important parameter during TIPS and that pros and cons of both methods should be carefully considered to obtain optimal material and TIPS process economy.

Keywords Thermally induced phase separation · Solvent removal method · Sound and heat insulation · Lyophilization · Extraction agent

✉ Juraj Kosek
Juraj.Kosek@vscht.cz

Patrik Boura
Patrik.Boura@vscht.cz

Alexandr Zubov
Alexandr.Zubov@vscht.cz

Bart Van der Bruggen
bart.vanderbruggen@kuleuven.be

[1] Department of Chemical Engineering, University of Chemistry and Technology Prague, Technická 5, Prague 6 166 28, Czech Republic

[2] Department of Chemical Engineering, KU Leuven, Celestijnenlaan 200F, Leuven B-3001, Belgium

1 Introduction

Nano and micro-cellular materials have various application possibilities in diverse fields of industry, with target applications significantly differing in their specific properties and required morphology. A common denominator for these applications, however, is that they require a high porosity. Such materials can be used as thermal or acoustic insulators [1–5], membranes [6–14], as support resins in solid phase synthesis [15, 16], as catalyst support [17] or as scaffolds in tissue engineering [18–27]. Polymeric porous materials are commonly divided into two categories based on their morphology: closed-cell and open-cell foams. Both of these have different characteristic properties and are usually manufactured by different preparation methods. Closed-cell structures generally have better heat insulation properties than open-cell structures and are commonly used as thermal insulators in construction industry. Open-cell materials have better sound insulation properties than closed-cell materials

[28] and, due to the interconnected porous structure, can be used as support in solid phase synthesis or scaffolds in tissue engineering. However, a thorough morphology description of such materials should include information about cell size, thickness of cell walls, cell spatial distribution, cell shape anisotropy and porosity.

Thermally induced phase separation (TIPS) [29–36], a versatile preparation method, can be utilized to produce either an open- or closed-cell morphology, or even a combination of both morphologies. TIPS generally consists of three consecutive steps: (1) homogenization of the polymer-solvent mixture, (2) temperature quench well below freezing point of the mixture, and (3) removal of the frozen solvent from the formed structure. The morphology of the formed heterophase material can be controlled by several parameters such as initial composition of polymer-solvent mixture, cooling rate and quenching temperature, the geometry of the experimental device and the evolution of temperature profile in the polymer–solvent mixture.It is, along with non-solvent induced phase separation (NIPS), one of the primary commercial porous membrane manufacturing methods [10]. Because the long-term industry goal is in engineering membranes with properties tailored to a desired application [9], it is essential to have an in-depth understanding of all the aforementioned steps of the TIPS manufacturing process.

The first reported TIPS experiments were conducted by Aubert and Clough [37], who dissolved polystyrene (PS) in either cyclohexane (CH) or benzene (B). Micro-structured foams were obtained after rapid cooling of homogenized PS-CH solutions with the initial PS concentrations near the critical concentration (φ_c) in the high-energetic region of the phase diagram under the spinodal curve. The frozen solvent was subsequently removed by freeze drying. Two different modes of solution demixing were observed, depending on the values of the mixture critical temperature (T_c) and freezing temperature (T_f) of the solvent: (1) liquid-liquid separation for the PS-CH system with T_c^{PSCH} higher than T_f^{CH}; (2) solid-liquid demixing for the PS-B system caused by T_f^B being higher than T_c^{PSB}, resulting in the premature freezing of the solvent and sheet-like morphology. Similar experiments with the PS-CH system were performed by Gao et al. [38]. , who studied the influence of the process conditions, such as the quenching temperature and the initial PS fraction, on the surface morphology of membranes prepared by TIPS. Gao et al. [38]. reported lower pore sizes with lower quenching temperature and spatial difference in the morphology with respect to the distance from the cooling plate. This was in contrast with the observations of Aubert and Clough [37], who reported a homogeneous morphology throughout the sample. The resulting porous membranes of Gao et al. [38]. exhibited a compact structure with small pores near the cooling plate and highly-porous interconnected structures near the side opposite to the cooling plate. The PS-CH system was afterwards studied by Vonka et al. [31]. to experimentally validate their Cahn-Hilliard model predictions of final foam morphologies based on process conditions.

The final morphology of polymeric foams prepared by TIPS is highly dependent on the initial concentration as demonstrated by Vonka et al. [31], as well as on molecular weight M_w of the polymer, as demonstrated by Cahn et al. [39]. Cooling the polymer solution by cooling agents at lower temperatures speeds up the cooling, stops phase separation (i.e., pore size evolution) earlier by freezing, resulting in smaller pore sizes and vice versa [40]. However, despite extensive studies of TIPS and influence of its process conditions, there have been - to the best of our knowledge - practically no studies comparing influence of the two solvent removal methods: (1) lyophilization [41, 42], and (2) extraction [38, 43–52] on the material morphology. The exceptions are the studies of Gao et al. [38]. , Matsuyama et al. [53] and Yang et al. [54], who observed some effects of solvent removal method on membrane morphology. Gao et al. [38] performed image analysis focused on the surface of two membrane samples with differently removed solvent at one set of conditions suggesting the influence of the solvent removal method. Matsuyama et al. [53] removed mineral oil from polyethylene membranes using different extraction agents and drying conditions, and measured membrane shrinkage. Matsuyama et al. [53] suggested that higher boiling point temperatures, i.e., slower evaporation, and higher extraction agent surface tension leads to more extensive shrinkage. Yang et al. [54] came to the conclusion that extraction of the solvent can lead to higher crystallinity. However, their experiments do not shed light on the bulk structure, as they have studied thin membranes and bulk morphology tends to differ in comparison to the surface morphology [30].

Materials with low heat conductivity are needed in various industries due to their important energy conservation role [55]. As demonstrated by Notario [3], lower foam pore sizes can lead to a lower thermal conductivity and according to Ferkl et al. [2], a reduction of pore sizes even below 100 μm is sufficient for thermal conductivity lowering effects. Preparation of foams by thermally induced phase separation can generally lead to foams with pore sizes below this threshold, potentially leading to enhanced thermal insulation. As mentioned above, open-cell foams can be used for sound insulation purposes, though their thermal insulation properties are inferior to closed-cell foams. In theory, sufficient pore size reduction could lower thermal conductivity of open-cell foams leading to the preparation of a unique material providing both thermal and sound insulation in one layer instead of two. Therefore, the thermal conductivity of

our foams was measured to investigate the potential application opportunity.

Effects of freeze-drying, i.e., lyophilization, are extensively studied in the field of food industry as a superior food preservation technique. It has been shown by Oikonomopoulou et al. [56] that different conditions of food freeze-drying lead to structural changes in porosity as well as pore sizes. The porous morphology might be similarly influenced by lyophilization during preparation by TIPS. On the other hand, solvent removal by an extraction agent could lead to structural changes due to the presence of low amounts of liquid solvent during the process.

To expand the knowledge about the possibly crucial influence of solvent removal methods on the bulk morphology, the influence of extraction and lyophilization was studied at different initial PS concentrations and solvent removal temperatures (T_r); both qualitative (SEM) and quantitative (mercury intrusion porosimetry) characterization methods were used.

2 Experimental procedures

2.1 Foaming procedure

An in-house built apparatus was used for preparation of samples, and it is schematically presented in Fig. 1. The foaming vessel (cf. Figure 1a) consists of a stainless-steel vessel (D) with a screw for the attachment to the stainless-steel top (A) and with a flange to attach bottom copper sheet (F). Between the top and the bottom part of the vessel two O-rings (C, E) ensure the sealing. This arrangement allows mostly one-dimensional heat transfer during the phase separation process 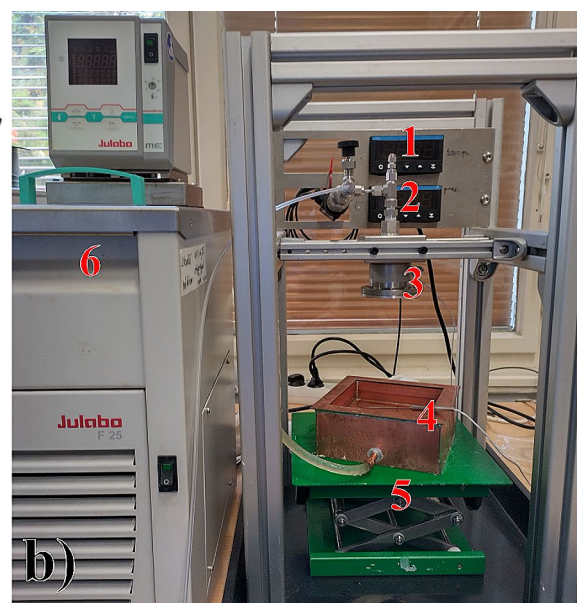due to the significantly more thermally conductive copper bottom sheet in comparison to the rest of the vessel made from the stainless-steel [57]. During the freezing the solution shrinks and if the heat transfer takes place in more than one dimension, voids and cracks can occur [37]. A teflon cylinder (B) can be used as an additional insulation. However, that significantly decreases the diameter of the samples and was not used in this work. The top (A), on which the vessel is screwed on, was connected to a temperature and pressure sensor, and a vacuum oil pump. The custom-made foaming apparatus (cf. Figure 1b) allows temperature control of the polymer-solvent system in foaming vessel (3) by submersion in hollow-walled cooling bath (4) connected to cryostat (6).

The samples were prepared at different solvent removal temperature (T_r), therefore the foaming procedure slightly varies at individually set conditions and it consists of several steps:

(1) A glass tube containing PS pellets and cyclohexane was placed into a preheated water bath kept at 50 °C to obtain a homogeneous solution.

(2) 7 ml of the homogeneous solution was poured into the foaming vessel, which was preheated to 50 °C in order to prevent premature cooling and phase separation.

(3) The vessel with the solution was then evacuated for approximately 10 s in order to remove the air entrapped in the solution due to dissolution during mixing and transfer from the tube to the foaming vessel and to remove the remaining air in the vessel [38].

(4) To start the foaming process, the bottom sheet of the foaming vessel was immersed in the cooling bath, thus lowering the temperature of the vessel by heat transfer through the bottom sheet and slowing down the side heat transfer. The cooling bath was prepared from ethanol as

Fig. 1 (**a**) Design of the foaming vessel. A – vessel top, B – insulating Teflon cylinder, C + E – sealing O-rings, D – stainless steel vessel, F – copper sheet. (**b**) The custom-made foaming apparatus. The main parts of the apparatus are: 1 – temperature display, 2 – pressure display, 3 – foaming vessel, 4 – bath with cooling medium, 5 – adjustable platform, 6 – cryostat. Partially adapted from Vonka et al. [31]

the heat transfer liquid and dry ice as the cooling agent, keeping the cooling bath temperature around −78.5 °C, the sublimation temperature of CO_2 [58].

(5) During the cooling, the PS–CH mixture separates into the polymer-rich phase and polymer-lean phase.

(6) At the temperature of 6.5 °C pure cyclohexane freezes [38, 59]. The addition of PS into CH lowers the freezing point by approximately 0.5 °C. The temperature of the solution inside the vessel is lowered below 6 °C within less than 3 min, creating thus solid PS porous structure filled with solid CH solvent.

(7) CH removal by either (a) lyophilization or (b) extraction at solvent removal temperature (T_r) 1 °C and 6 °C.

(7a) The temperature sensor was inserted into the bottom sheet to measure the temperature near the sample.

(8a) The solvent was then removed by the freeze-drying method, maintaining T_r and evacuating the vessel until the pressure inside decreased below 1 Pa, marking the end of sublimation, which took around 3.5 h (at 1 °C) or 2 h (at 6 °C), respectively.

(7b) The frozen sample was removed from the foaming vessel and transferred into the beaker filled with n-butanol, precooled just below T_r, where n-butanol acts as a CH extraction agent. The beaker was then covered with a Petri dish and transferred into the fridge maintaining T_r.

(8b) Extraction of CH led to the occurrence of two visually slightly different liquid phases in the beaker, cf. Figure 2.

(9b) The major part of the extraction agent was exchanged once a day and the mixing of the solution was facilitated by occasional gentle shaking of the beaker in order to accelerate the extraction process. This step was repeated for approximately 6 days (at 1 °C) or 3 days (at 6 °C), until the solution in the beaker stayed visually homogeneous, marking the end of the extraction process.

(10b) The sample was removed from the extraction agent and left to dry in a ventilated environment at room temperature.

Out of the four preliminary tested extraction agents, namely: methanol, ethanol, n-propanol and n-butanol, the fastest extraction, at our conditions, occurred while employing n-butanol, which was therefore used for further experiments. We attribute this to n-butanol having the lowest polarity out of the tested alcohols, resulting in comparatively higher affinity to non-polar cyclohexane, as well as the highest density, higher than the density of cyclohexane, prompting cyclohexane rich phase to rise and thus facilitate the extraction process.

2.2 Characterization methods

The properties of the prepared samples were characterized by various characterization methods. To visualize structure of the samples, Scanning Electron Microscopy (SEM) was employed.

SEM was performed on VEGA 3 SBU, Tescan electron microscope, backscattered electron (BSE) mode, (high voltage) HV = 20 kV. All polymer samples have been coated with a layer of gold prior to the SEM measurement.
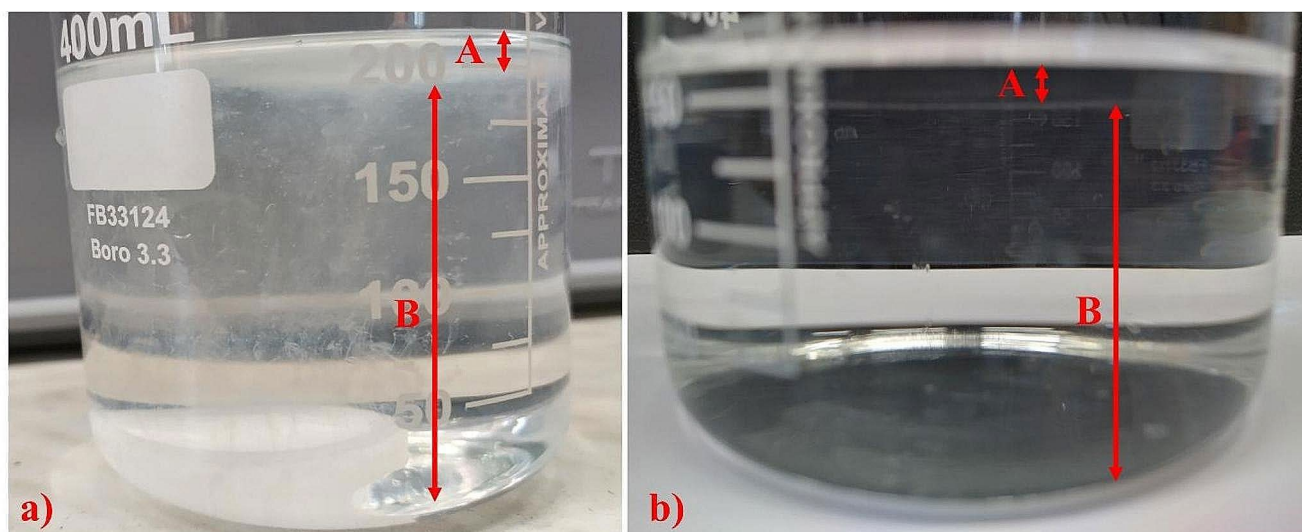

Fig. 2 Photos of two visually slightly different liquid phases during extraction taken at room temperature: (**a**) with solid PS-CH, (**b**) without solid PS-CH. CH rich phase is represented by A while n-butanol rich phase is represented by B. The photos were taken at room temperature, a higher temperature compared to our foaming procedure, to achieve better visibility, i.e., in the absence of water condensation, and example **a**) would not lead to the successful creation of porous structure due to too high temperature of extraction

Visualization by computational micro X-ray tomography method was tested, but its resolution (ca. 2 μm) proved to be too low to visualize morphology of the samples.

The porosity of the samples was determined from measured volume (m_{sample}) and weight (m_{sample}) of the prepared samples based on the knowledge of polystyrene bulk density ρ_{PS} as follows:

$$x = (1 - m_{sample}/V_{sample}/\rho_{PS})\ 100\% \tag{1}$$

and to further characterize the foam morphology quantitatively, Quantachrome PoreMaster 33 was employed to characterize the samples by low- and high-pressure mercury intrusion porosimetry (MIP) reaching pressure up to 414 MPa and allowing pore size determination in the range from 1 mm down to 3 nm. The results of mercury porosimetry are interpreted with a caution because the sample compression can affect the results.

Additionally, the thermal conductivity of samples was measured by Transient Hot Bridge (THB) method using Linseis THB 100. It is a device convenient for very fast measurements (approximately 10 min for solids) with thermal conductivities in the range from 0.01 to 100 W·m^{-1}·K^{-1} with 2% uncertainty [60]. The hot point type sensor was used in between two identical samples; an averaged thermal conductivity was measured with samples facing both top and bottom sides.

2.3 Materials

Polystyrene (PS) foams were prepared from commercial PS pellets from the Sigma Aldrich (Merck) with molecular weight M_w = 280 kDa, density ρ_{PS} = 1047 kg/m^3 and glass transition temperature T_g = 100 °C. Cyclohexane (CH, 99% purity) was used as a solvent, n-butanol (99.5% purity, $\rho_{n-butanol}$ = 810 kg/m^3) was used as an extraction agent, both purchased from PENTA, Prague - Czech Republic. Methanol (99.5% purity, $\rho_{methanol}$ = 790 kg/m^3), ethanol (96% purity, $\rho_{ethanol}$ = 810 kg/m^3), n-propanol (95.5% purity, $\rho_{n-propanol}$ = 800 kg/m^3), all purchased from LACH-NER, s.r.o., Neratovice - Czech Republic, were preliminary tested as extraction agents. The initial PS fraction in the foaming solution was 12 and 14 wt% (9.2 and 10.8 vol%, respectively) as shown in Fig. 3. These concentrations were chosen for two reasons: (i) the concentration had to be high enough to prepare mechanically stable foams, as lower fractions of PS caused foam fragility, and (ii) it had to be low enough in order to ensure prevalent separation by spinodal decomposition and thus to obtain an interconnected porous structure. The initial solution was preheated to the initial temperature T_{init} = 50 °C and then cooled down in a bath with dry ice kept at the cooling temperature T_{cool} = -78.5 °C.

Fig. 3 PS/CH phase diagram, with depicted PS concentrations used for foam preparation. Adapted from Vonka et al. [31]
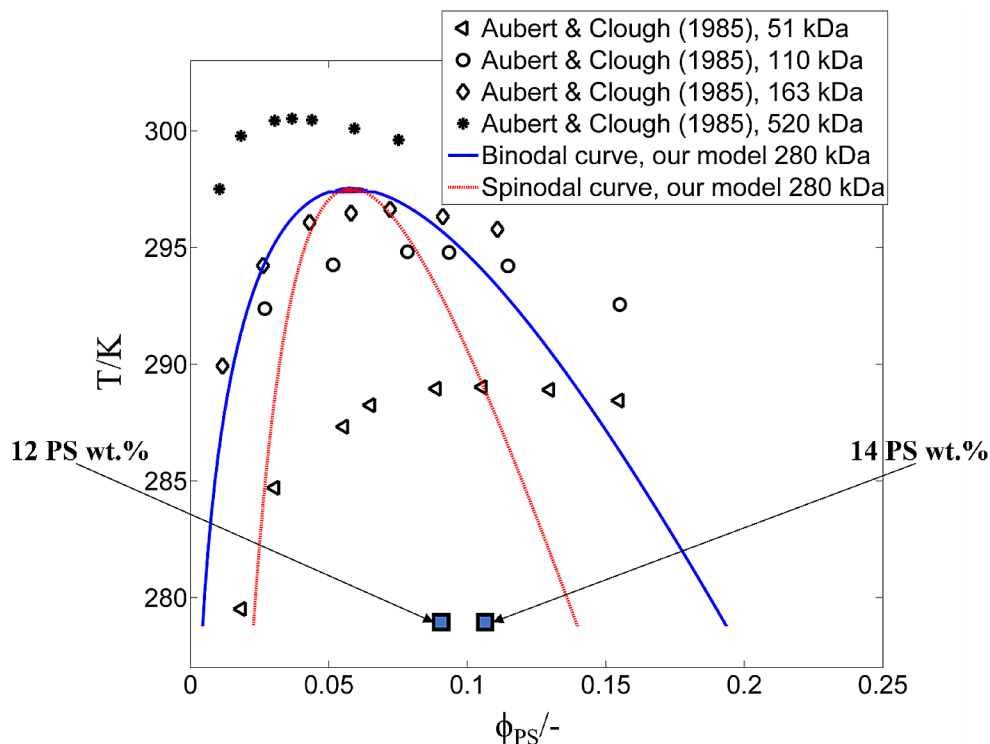
3 Results and discussion

3.1 Structure visualization

Samples were cut prior to the SEM characterization to enable visualization of the bulk structure. However, a foam structure tends to wrap during the cutting. Therefore, the foam was cooled by liquid nitrogen and cut by a surgical knife to avoid destruction of the structure as much as possible. Furthermore, cuts from the middle of the sample were used in order to show the structure developed without influence of the horizontal heat transfer through the walls. In Fig. 4, SEM images are shown for four foams prepared from solutions containing 12 wt% of PS (cf. Figure 4a, b) and 14 wt% of PS (cf. Figure 4c, d) prepared by solvent removal at 6 °C (CH melting temperature $T_{mCH} \approx 6.5$ °C). Foams depicted on the left side (cf. Figure 4a, c) were prepared using extraction as a solvent removal method and on the right side (Fig. 4b, d) are foams after lyophilization. Qualitatively, all foams have an interconnected, partially closed porous structure. By comparing left and right side of Fig. 4, it can be concluded that the solvent removal method considerably influences the morphology. According to SEM images, foams prepared using lyophilization seem to have significantly larger pores than foams prepared using an extraction agent. Furthermore, foams prepared by lyophilization seem to have thicker cell walls compared to foams after the use of an extraction agent. A larger average wall thickness and pore size after lyophilization compared to

Extraction   Lyophilization

Fig. 4 SEM visualization of PS foams morphologies prepared from PS/CH solutions containing 12 and 14 PS wt% using different solvent removal methods at solvent removal temperature $T_r = 6$ °C as follows: (**a**) 12 PS wt% - extraction; (**b**) 12 PS wt% - lyophilization; (**c**) 14 PS wt% - extraction; (**d**) 14 PS wt% -lyophilization

solvent removal by extraction agent could be the result of a destruction of thin walls in the lyophilized samples creating larger pores and leaving mostly thicker walls. This phenomenon is visually indicated by the 12 PS wt% lyophilized sample (cf. Figure 4b), where several residues of thin walls seem to be left.

3.2 Pore size distribution

The influence of the solvent removal method and temperature T_r, and the initial PS wt% on the pore size distribution was studied using MIP. Sample cuts for MIP were taken from the centre of nitrogen cooled samples, while the volume percentage pore distribution was averaged from measurements of at least two samples for each combination of preparation parameters.

In Fig. 5 the influence of the PS wt% on the pore size distribution, at $T_r = 1$ °C and 6 °C, is presented. At $T_r = 6$ °C, pore diameters of 14 PS wt% foams were generally smaller compared to 12 PS wt% foams after solvent removal by both extraction and lyophilization, in agreement with commonly observed TIPS trends of decreasing pore sizes with increasing PS wt%. Additionally, 14 PS wt% foams had a more narrow pore distribution compared to 12 PS wt% foams, allowing a better control of pore size. Both effects were much more significant when using lyophilization in comparison to extraction. At $T_r = 1$ °C, the same trends occur with a comparatively smaller effect of the PS wt% when lyophilizing the samples, suggesting worse structure damage resistance of 12 PS wt% at higher $T_r = 6$ °C. Supported by the high volatility of CH, such damage might be caused by rapid volumetric gas expansion in pores caused by solvent phase change from solid to gaseous state. Larger pore sizes were obtained after twice slower extraction at lower temperature, indicating influence of a long-term effects pointing towards Ostwald ripening. CH is slowly exchanged by lower surface tension n-butanol, causing larger difference between surface tensions of pore filing and pore walls, leading to slow minimalization of the specific surface pore area (i.e., larger pore sizes).

A comparison of solvent removal methods at different PS wt%, at $T_r = 1$ °C and 6 °C, is made in Fig. 6. The measurement confirms the qualitative observation using SEM that the lyophilized foams have significantly larger pore diameters than the extracted foams prepared at the same conditions. Moreover, the measurements show that the solvent removal method can have an even greater influence on the pore size than the PS wt%, the effect being more significant at 12 PS wt% and $T_r = 6$ °C. As this effect is greatly diminished at $T_r = 1$ °C for 12 PS wt%, it indicates that at $T_r = 6$ °C the thinner cell walls might be destroyed during the lyophilization due to process conditions too close to T_m
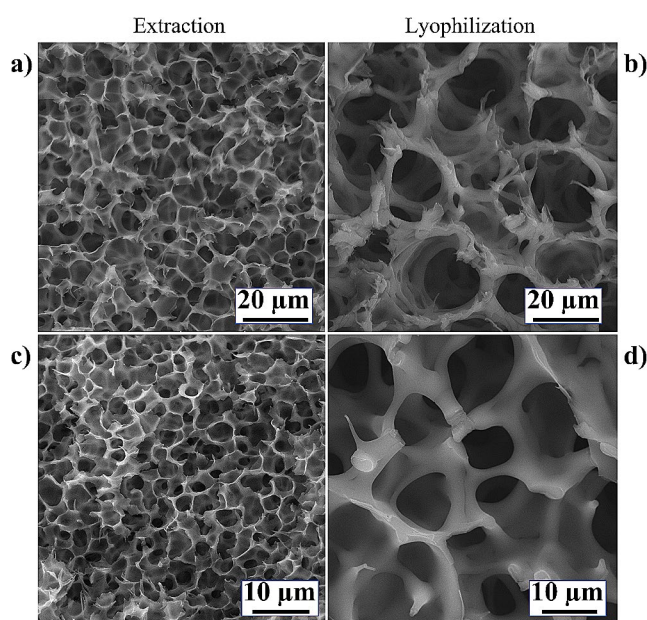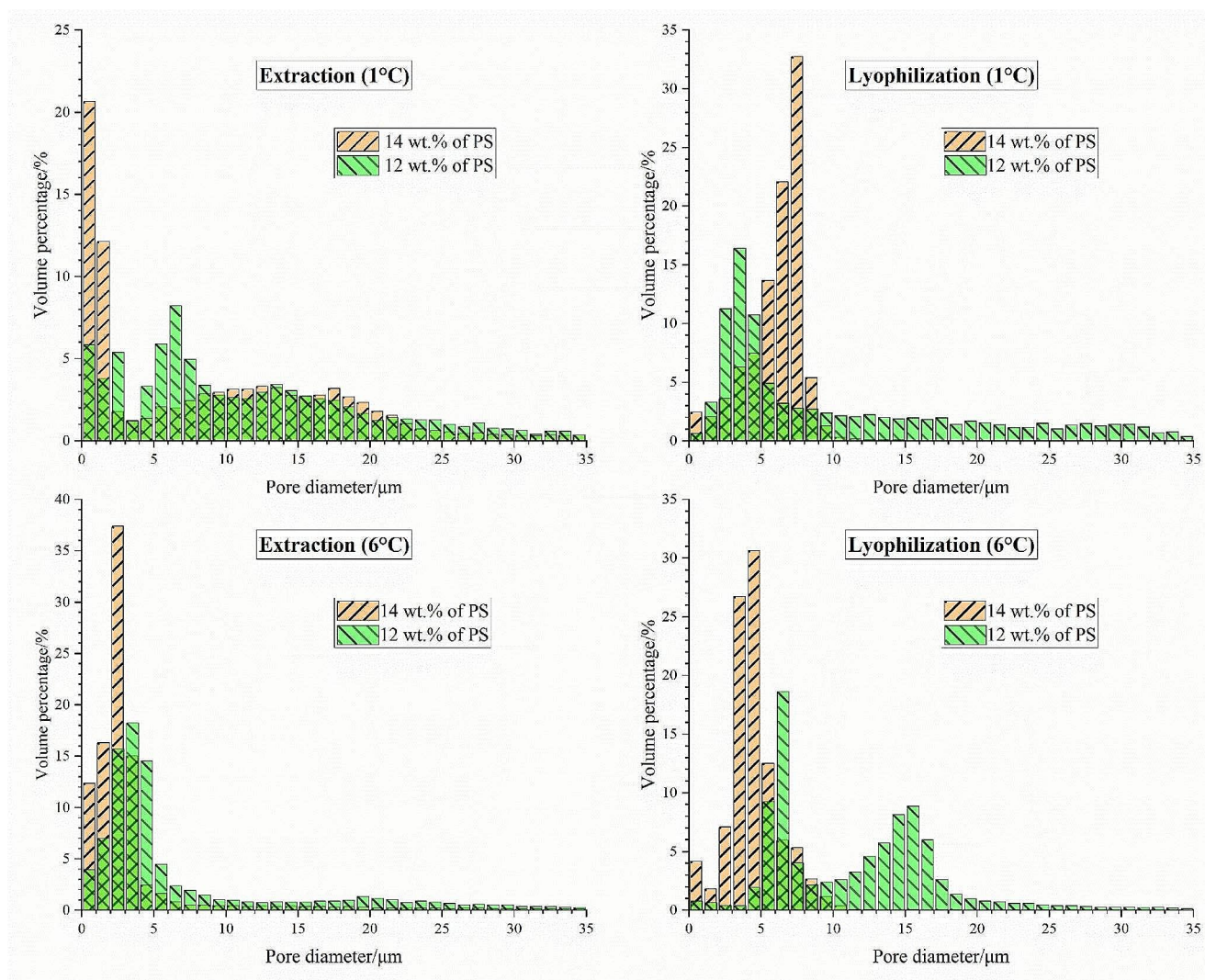
Fig. 5 Comparison of PS wt% influence on volume percentage pore distribution using either extraction or lyophilization as a solvent removal method at $T_r = 1$ °C and 6 °C; combination of the two colours signifies overlap

of the solvent, and thus due to its presence in liquid form during lyophilization. Overall, the results regarding the pore size distribution are opposite to those of Gao et al. [38]. , who observed smaller pores using lyophilization at 8.7 vol% of PS during membrane preparation. However, in comparison to the preparation method reported here, Gao et al. have used ethanol instead of butanol as an extraction agent and have done only qualitative visual characterization of the membrane surface. Therefore, our sample characterization is more detailed, at least regarding the bulk morphology of foams prepared by thermally induced phase separation.

Pore size can be potentially influenced by solvent expansion during solidification, nevertheless CH on the contrary increases its density during solidification causing volume contraction and this would occur prior to the solvent removal. Reaching generally smaller pore sizes using extraction agent can be explained by the effects of foam

contraction caused by the extraction agent during the drying process at room temperature leading to a pore size shrinking as observed on membrane samples by Matsuyama et al. [53], who observed a decreased porosity as well, suggesting pore collapse caused by capillary forces. The apparent drawback of solvent removal by extraction agent, apart from longer process duration, is the broad pore size distribution, which is at least partially caused by the generally more difficult process control and in essence lower repeatability leading to the broader pore size distribution.

3.3 Porosity

The porosity of the samples was measured both by MIP and from volume/mass measurements as described above in Sect. 2.2. The results from both methods do not show a significant deviation from each other and therefore the porosity
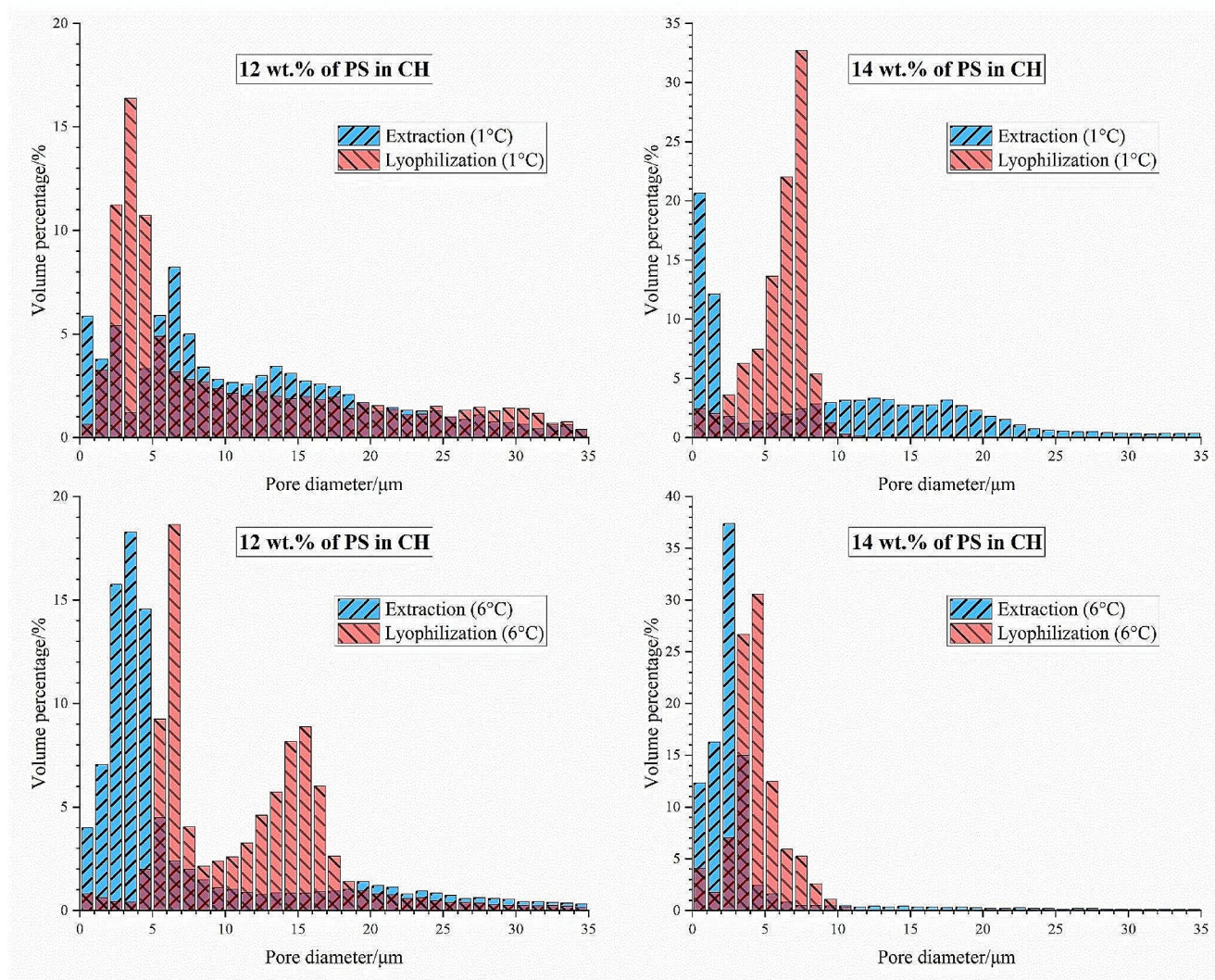
Fig. 6 Comparison of solvent removal method influence $T_r = 1$ °C and 6 °C on volume percentage pore distribution at 12 and 14 wt% of PS in initial PS-CH solution; combination of the two colours signifies overlap

Table 1 Averaged porosities of PS foams prepared at different conditions

T_r/°C	PS wt%	Solvent removal method	
		Lyophilization	Extraction
		Porosity/%	
6	12	84.0 ± 2.0	79.3 ± 5.4
6	14	83.9 ± 0.8	72.1 ± 13.1
1	12	85.5 ± 0.9	79.0 ± 0.4
1	14	82.6 ± 0.5	74.0 ± 3.3

of the PS foams at different conditions was averaged using results from both methods. As shown in Table 1, the porosity results support the pore size distribution results, showing lower porosities after the use of an extraction agent, as well as the generally higher standard deviation, reaching up to 13.1%, caused by the more difficult process control compared to lyophilization. Furthermore, lower porosities were

measured at higher 14 PS wt% which is understandable due to the higher polymer content in the initial solution.

3.4 Thermal conductivity

All prepared PS foam samples have a thermal conductivity λ slightly above 0.040 $W \cdot m^{-1} \cdot K^{-1}$ with minimal deviation (cf. Table 2). In comparison, commercially available expanded polystyrene (EPS) has a thermal conductivity typically between 0.035 and 0.037 $W \cdot m^{-1} \cdot K^{-1}$ at 10 °C [61]. However, the thermal conductivity of PS increases with temperature up to its glass transition temperature $T_g \approx 90$ °C [62], thus a better comparison can be achieved by comparing specific commercially available product e.g. Styrodur® 3035, extruded polystyrene (XPS) produced by BASF SE, Germany, with a thermal conductivity in the range from 0.036 to 0.037 $W \cdot m^{-1} \cdot K^{-1}$ at 20 and 30 °C respectively

Table 2 Average thermal conductivities of selected foams prepared at $T_r = 6\ °C$

Solvent removal method	PS wt%	Porosity	λ measured at temperature/°C	Thermal conductivity $\lambda/W{\cdot}m^{-1}{\cdot}K^{-1}$
Lyophilization	12%	85.1 ± 1.9	26.3 ± 0.1	0.0408 ± 0.0013
	14%	83.9 ± 0.8	25.4 ± 1.1	0.0401 ± 0.0012
Extraction	12%	84.2 ± 0.4	25.3 ± 0.1	0.0402 ± 0.0012
	14%	85.2 ± 2.8	26.9 ± 1.3	0.0428 ± 0.0012

[63]. Additionally, commercially available heat insulation foams have a porosity around 95 to 98% [61]. There is still some room for a thermal conductivity decrease through an increase of porosity by the modification of the preparation process. Furthermore, as the foams prepared in this study have mostly interconnected pores, they should have remarkably better acoustic insulation properties in comparison to EPS. Acoustic insulation properties should also significantly increase with decreasing pore size [4, 28]; the newly developed PS foams potentially provide both reasonable thermal insulation and superb acoustic insulation properties in one layer of insulation.

4 Conclusions

The influence of the solvent removal method on the bulk morphology of polymeric porous materials prepared by thermally induced phase separation (TIPS) was studied. A well described PS/CH system was employed in order to study the influence of solvent removal by lyophilization in comparison to an extraction agent (*n*-butanol). Prepared foams were characterized both qualitatively and quantitatively comparing their pore size distribution, structure, porosity, and thermal conductivity.

Qualitatively, all of the foams were found to have an interconnected partially closed pore structure. A significant influence of solvent removal method was observed, as average pore sizes of prepared foams were approximately two times larger after lyophilization at solvent removal temperature T_r near solvent melting temperature T_m in comparison to foams of respective PS wt% after solvent removal by an extraction agent. This effect was decreased at lower temperature, however not entirely diminished. On the other hand, the porosity of the samples was measured to be above 82% for lyophilized samples with minimal deviation on the contrary to the samples after the application of extraction agent, which have generally shown a decrease in porosity up to 10% for samples from 14 PS wt% at 6 °C, suggesting a decrease in both pore size and porosity due to foam contraction. This work therefore proves that the solvent removal method is an important parameter during TIPS and that the above mentioned effects should be considered, while using

lyophilization as a solvent removal method together with economics of both methods as lower temperature leads to a longer solvent removal process and higher cooling costs, while the use of an extraction agent arguably offers a better scale up option as well as lower pore sizes in exchange for the decrease in porosity.

All prepared PS foams had a thermal conductivity (λ) slightly above $0.040\ W{\cdot}m^{-1}{\cdot}K^{-1}$ at 26 °C. This value is about 10 to 15% higher than that of the commercially available EPS, which have a porosity typically in the range of 95 to 98%. There is some room for improvement, as foam porosity could be further increased by preparation process modification, e.g., by combination with other foaming approaches, leading to an associated λ decrease due to the increase in porosity. Furthermore, as the newly prepared foams have mostly interconnected pores, they should have notably better acoustic insulation properties in comparison to EPS. Acoustic insulation properties should also significantly improve with decreasing pore size, so that our PS foams can potentially provide both reasonable thermal insulation and superb acoustic insulation properties in one layer of insulation. This is an example of one of the possible applications, as an insulation, while TIPS allows tailored preparation, adjusting the process parameters, to obtain a material with desired morphology for various target applications. This opens a possible window for target design and optimization of commercially produced nano- and microstructured materials taking into account the influence of the solvent removal method.

Author contributions P. B.: Writing - Original Draft, Investigation, Formal analysis, Validation, Methodology, Data Curation, Software. A. Z.: Supervision, Project administration, Writing - Review & Editing, Software. B. V. d. B.: Supervision, Conceptualization, Writing - Review & Editing. J. K.: Project administration, Supervision, Funding acquisition, Writing - Review & Editing, Resources, Conceptualization.

Data availability Data sets generated during the current study are available from the corresponding author on reasonable request.

Declarations

References

1. P. Ferkl, M. Toulec, E. Laurini et al., Chem. Eng. Sci. **172**, 323 (2017). https://doi.org/10.1016/j.ces.2017.06.035
2. P. Ferkl, R. Pokorný, M. Bobák, J Kosek, Chem. Eng. Sci. **97**, 50 (2013). https://doi.org/10.1016/j.ces.2013.04.018
3. B. Notario, J. Pinto, E. Solorzano, J.A. de Saja, M. Dumon, M.A. Rodríguez-Pérez, Polymer. **56**, 57 (2015). https://doi.org/10.1016/j.polymer.2014.10.006
4. S. Hu, J. Cai, G. Liao, Q Fu (2019) Adv Polym Tech 2019: 7608641. https://doi.org/10.1155/2019/7608641
5. A.N. Chen, F. Gao, M. Li et al., Ceram. Int. **45**, 15538 (2019). https://doi.org/10.1016/j.ceramint.2019.05.059
6. A.G. Mikos, A.J. Thorsen, L.A. Czerwonka et al., Polymer. **35**, 1068 (1994). https://doi.org/10.1016/0032-3861(94)90953-9
7. X. Zhang, H.N. Li, C.Y. Zhu, X.J. Huang, A. Greiner, Z.K. Xu, Chem. Eng. J. **434**, 9 (2022). https://doi.org/10.1016/j.cej.2022.134758
8. Y.H. Tang, Y.K. Lin, W.Z. Ma, X.L. Wang, J. Membr. Sci. **639**, 26 (2021). https://doi.org/10.1016/j.memsci.2021.119759
9. Y. Tang, Y. Lin, D.M. Ford et al., J. Membr. Sci. **640**, 119810 (2021). https://doi.org/10.1016/j.memsci.2021.119810
10. S.P. Nunes, P.Z. Culfaz-Emecen, G.Z. Ramon et al., J. Membr. Sci. **598**, 117761 (2020). https://doi.org/10.1016/j.memsci.2019.117761
11. Y. Guo, T. Zhang, M. Chen, C. Li, H. Wu, S. Guo, J. Membr. Sci. **619**, 118778 (2021). https://doi.org/10.1016/j.memsci.2020.118778
12. M. Liu, S. Liu, Z. Xu, Y. Wei, H. Yang, Front. Chem. Sci. Eng. **10**, 57 (2016). https://doi.org/10.1007/s11705-016-1561-7
13. J. Pan, L. Zhang, Z. Wang, S.-P. Sun, Z. Cui, N. Tavajohi, Front. Chem. Sci. Eng. **16**, 720 (2022). https://doi.org/10.1007/s11705-021-2098-y
14. T. Tsujimoto, T. Kitagawa, S. Yoneda, H. Uyama, J. Porous Mater. **24**, 233 (2017). https://doi.org/10.1007/s10934-016-0256-2
15. S. Zalipsky, J.L. Chang, F. Albericio, G. Barany, React. Polym. **22**, 243 (1994). https://doi.org/10.1016/0923-1137(94)90122-8
16. I. Coin, M. Beyermann, M Bienert, Nat. Protoc. **2**, 3247 (2007). https://doi.org/10.1038/nprot.2007.454
17. G. Wang, J. Wang, H. Zhang et al., Chem. Eng. J. **313**, 1607 (2017). https://doi.org/10.1016/j.cej.2016.11.032
18. C. Schugens, V. Maquet, C. Grandfils, R. Jerome, P Teyssie, Polymer. **37**, 1027 (1996). https://doi.org/10.1016/0032-3861(96)87287-9
19. J.M. Polak, S. Mantalaris, S.E. Harding, *Advances in Tissue Engineering* (Imperial College, 2008)
20. A.E. Erickson, J. Sun, S.K.L. Levengood et al., Biomed. Microdevices. **21**, 16 (2019). https://doi.org/10.1007/s10544-019-0373-1
21. A. Buzarovska, S. Dinescu, L. Chitoiu, M Costache, J. Mater. Sci. **53**, 11151 (2018). https://doi.org/10.1007/s10853-018-2415-0
22. L. Zhu, S. Chen, K. Liu et al., Chem. Eng. J. **391**, 123524 (2020). https://doi.org/10.1016/j.cej.2019.123524
23. S. Milovanovic, J. Pajnik, I. Lukic, J. Appl. Polym. Sci. **139**, 26 (2022). https://doi.org/10.1002/app.51839
24. Q.Q. Yao, Y. Liu, Y.N. Pan, J.M. Miszuk, HL Sun, J. Biomed. Mater. Res. Part. B **108**, 2699 (2020). https://doi.org/10.1002/jbm.b.34601
25. R. Zeinali, L.J. Valle, J. Torras, J Puiggali, Int. J. Mol. Sci. **22**, 46 (2021). https://doi.org/10.3390/ijms22073504
26. N. Hojat, P. Gentile, A.M. Ferreira, L Šiller, J. Porous Mater. **30**, 93 (2023). https://doi.org/10.1007/s10934-022-01309-y
27. A. Salerno, C. Domingo, J. Porous Mater. **22**, 425 (2015). https://doi.org/10.1007/s10934-015-9911-2
28. C. Zhang, J. Li, Z. Hu, F. Zhu, Y. Huang, Mater. Design. **41**, 319 (2012). https://doi.org/10.1016/j.matdes.2012.04.031
29. C.A. Martinez-Perez, I. Olivas-Armendariz, J.S. Castro-Carmona, P.E. Garcia-Casillas, *Scaffolds for Tissue Engineering Via Thermally Induced Phase Separation* (Intech Europe, Rijeka, 2011)
30. A. Nistor, M. Vonka, A. Rygl, M. Voclova, M. Minichova, J Kosek, Macromol. React. Eng. **11**, 1600007 (2017). https://doi.org/10.1002/mren.201600007
31. M. Vonka, A. Nistor, A. Rygl, M. Toulec, J Kosek, Chem. Eng. J. **284**, 357 (2016). https://doi.org/10.1016/j.cej.2015.08.105
32. D. Rusakov, A. Menner, F. Spieckermann, H. Wilhelm, A. Bismarck, J. Appl. Polym. Sci. **139**, 51423 (2022). https://doi.org/10.1002/app.51423
33. T.L. Tran, P.K. Chan, D. Rousseau, Chem. Eng. Sci. **60**, 7153 (2005). https://doi.org/10.1016/j.ces.2005.06.028
34. A. Bertei, B. Tellini, R Mauri, Chem. Eng. Sci. **203**, 450 (2019). https://doi.org/10.1016/j.ces.2019.04.014
35. H. Manzanarez, J.P. Mericq, P. Guenoun, J. Chikina, D. Bouyer, Chem. Eng. Sci. **173**, 411 (2017). https://doi.org/10.1016/j.ces.2017.08.009
36. O.C. Onder, E. Yilgor, I. Yilgor, J. Polym. Sci. Pol. Phys. **57**, 98 (2019). https://doi.org/10.1002/polb.24762
37. J.H. Aubert, RL Clough (1985) Polymer 26: 2047. https://doi.org/10.1016/0032-3861(85)90186-7
38. C.Y. Gao, A. Li, L.X. Feng, X.S. Yi, J.C. Shen, Polym. Int. **49**, 323 (2000). https://doi.org/10.1002/(SICI)1097-0126(200004)49:4%3C323::AID-PI369%3E3.0.CO;2-7.
39. JW Cahn, Acta Metall. Mater. **9**, 795 (1961). https://doi.org/10.1016/0001-6160(61)90182-1
40. K.S. McGuire, A. Laxminarayan, DR Lloyd, Polymer. **36**, 4951 (1995). https://doi.org/10.1016/0032-3861(96)81620-x
41. S.-W. Song, J.M. Torkelson, Macromolecules. **27**, 6389 (1994). https://doi.org/10.1021/ma00100a024
42. R.M. Hikmet, S. Callister, A. Keller, Polymer. **29**, 1378 (1988). https://doi.org/10.1016/0032-3861(88)90299-6
43. Ö.C. Önder, E. Yilgör, I Yilgör, Polymer. **107**, 240 (2016). https://doi.org/10.1016/j.polymer.2016.11.025
44. F.C. Pavia, V.L. Carrubba, V Brucato (2012) AIP Conference Proceedings 1459: 51. https://doi.org/10.1063/1.4738395
45. V.L. Carrubba, F. Pavia, V. Brucato, S Piccarolo, Int.J. Mater. Form. **1**, 619 (2008). https://doi.org/10.1007/s12289-008-0332-5
46. M.R. Caplan, C.-Y. Chiang, D.R. Lloyd, L.Y. Yen, J. Membr. Sci. **130**, 219 (1997). https://doi.org/10.1016/S0376-7388(97)00027-6
47. R.H. Mehta, D.A. Madsen, D.S. Kalika, J. Membr. Sci. **107**, 93 (1995). https://doi.org/10.1016/0376-7388(95)00106-M
48. G.B.A. Lim, S.S. Kim, Q. Ye, Y.F. Wang, D.R. Lloyd, J. Membr. Sci. **64**, 31 (1991). https://doi.org/10.1016/0376-7388(91)80075-H
49. S.S. Kim, D.R. Lloyd, J. Membr. Sci. **64**, 13 (1991). https://doi.org/10.1016/0376-7388(91)80074-G
50. F.J. Tsai, JM Torkelson, Macromolecules. **23**, 775 (1990). https://doi.org/10.1021/ma00205a014
51. D.R. Lloyd, K.E. Kinzer, H.S. Tseng, J. Membr. Sci. **52**, 239 (1990). https://doi.org/10.1016/S0376-7388(00)85130-3

52. G.T. Caneba, DS Soong, Macromolecules. **18**, 2538 (1985). https://doi.org/10.1021/ma00154a031

53. H. Matsuyama, M. Kim, D.R. Lloyd, J. Membr. Sci. **204**, 413 (2002). https://doi.org/10.1016/s0376-7388(02)00052-2

54. M.C. Yang, J.S. Perng, J. Polym. Research-Taiwan. **6**, 251 (1999). https://doi.org/10.1007/s10965-006-0095-y

55. W. Suthabanditpong, C. Takai, H. Razavi-Khosroshahi, Y. Okada, M.S. El-Salmawy, M. Fuji, Adv. Powder Technol. **30**, 207 (2019). https://doi.org/10.1016/j.apt.2018.10.024

56. V.P. Oikonomopoulou, M.K. Krokida, VT Karathanos, Procedia Food Sci. **1**, 647 (2011). https://doi.org/10.1016/j.profoo.2011.09.097

57. Engineers, Edge, Thermal Properties of Metals, Conductivity, Thermal Expansion, Specific Heat - Engineers Edge, https://www.engineersedge.com/properties_of_metals.htm (Accessed March 15th 2024)

58. CR Barber, Br. J. Appl. Phys. **17**, 391 (1966). https://doi.org/10.1088/0508-3443/17/3/312

59. T.F. Sun, P.J. Kortbeek, S.N. Biswas, N.J. Trappeniers, J.A. Schouten, Berichte Der Bunsengesellschaft für Phys. Chemie. **91**, 1013 (1987). https://doi.org/10.1002/bbpc.19870911008

60. U. Hammerschmidt, V. Meier, Int. J. Thermophys. **27**, 840 (2006). https://doi.org/10.1007/s10765-006-0061-2

61. Expanded Polystyrene (EPS), Ultimate Guide on Foam Insulation Material https://omnexus.specialchem.com/selection-guide/expanded-polystyrene-eps-foam-insulation (Accessed March 15th 2024)

62. WN, J.A. dos Santos, R.G. de Sousa, Polym. Test. **32**, 987 (2013). https://doi.org/10.1016/j.polymertesting.2013.05.007

63. S.E. BASF, R. Technical Data, Applications, Assistance Data for Dimensioning, PMFS 1431 BE, https://static1.squarespace.com/static/53f9d90ee4b0572e560769f8/t/5717a16755598683056d7eed/1461166443509/styrodur_technical_data.pdf (Accessed March 15th 2024)